TU Delft

Delft University of Technology

The effect of cutting tool coating on the form and dimensional errors of machined holes in GLARE (R) fibre metal laminates

Giasin, K.; Hawxwell, J.; Sinke, J.; Dhakal, H.; Köklü, U.; Brousseau, E.

DOI
10.1007/s00170-020-05211-2

Publication date
2020

Document Version
Final published version

Published in
International Journal of Advanced Manufacturing Technology

Citation (APA)
Giasin, K., Hawxwell, J., Sinke, J., Dhakal, H., Köklü, U., & Brousseau, E. (2020). The effect of cutting tool coating on the form and dimensional errors of machined holes in GLARE (R) fibre metal laminates. *International Journal of Advanced Manufacturing Technology*, *107*(5-6), 2817-2832. https://doi.org/10.1007/s00170-020-05211-2

Important note
To cite this publication, please use the final published version (if applicable).
Please check the document version above.

Copyright
Other than for strictly personal use, it is not permitted to download, forward or distribute the text or part of it, without the consent of the author(s) and/or copyright holder(s), unless the work is under an open content license such as Creative Commons.

Takedown policy
Please contact us and provide details if you believe this document breaches copyrights.
We will remove access to the work immediately and investigate your claim.

This work is downloaded from Delft University of Technology.
For technical reasons the number of authors shown on this cover page is limited to a maximum of 10.

The International Journal of Advanced Manufacturing Technology (2020) 107:2817–2832
https://doi.org/10.1007/s00170-020-05211-2

ORIGINAL ARTICLE

The effect of cutting tool coating on the form and dimensional errors of machined holes in GLARE® fibre metal laminates

K. Giasin[1] · J. Hawxwell[2] · J. Sinke[3] · H. Dhakal[1] · U. Köklü[4] · E. Brousseau[5]

Received: 16 May 2019 / Accepted: 13 March 2020 / Published online: 27 March 2020
© The Author(s) 2020

Abstract

Fibre metal laminates (FMLs) are multilayered metal composite materials currently used in aeronautical structures, especially where fatigue and impact resistance are required. FMLs are produced in large panels and often require assembly using the drilling process for riveting purposes. Hole making is a critical machining process in the joining and assembly of aeronautical components, which has to meet stringent tolerance requirements. This paper reports a systematic analysis of hole integrity when drilling an FML known as GLARE®. In particular, the primary objective is to investigate the impact of three different drill coatings (TiAlN, TiN and AlTiN/TiAlN), against several important hole parameters: thrust force, hole size, circularity, cylindricity and perpendicularity. The results show that TiAlN-coated drills produced the highest thrust force, while TiN-coated drills produced holes with the lowest deviation between the hole diameter measured at the entry and the exit and that the drill coating was the most influential parameter for the resulting hole size. TiAlN-coated drills resulted in the highest circularity at the upper part of the hole, while hole cylindricity tended to be best when using AlTiN/TiAlN- and TiN-coated drills. The ANOVA analysis shows that the drill coating and the spindle speed had a significant influence on hole size and circularity, while drill coating was the only influential parameter on hole cylindricity, and spindle speed was the only contributing parameter on hole perpendicularity. Finally, scanning electron microscopy analyses showed two distinct hole wall surface damage phenomenon due to broken fibres and evacuated metallic chips.

Keywords Drilling · Thrust force · Coatings · Hole size · Circularity · Cylindricity · Perpendicularity · Glare®

1 Introduction

Drilling is a conventional machining process for producing round holes of different sizes and depths in aeronautical structures. The number of holes can vary from 300,000 up to three million in commercial aircraft [1–4]. At the same time, poor hole quality is responsible for around 60% of all parts rejection [1, 5, 6]. Poorly machined holes usually lead to costly corrective manufacturing measures and increase the required inspection time [3, 4, 7]. Holes are produced to allow for fastener installation for assembly purposes. Failure to produce acceptable hole quality can lead to excessive preloads, fatigue and may cause cracks in the assembly. Hole quality is often evaluated by several parameters which must meet

✉ K. Giasin
khaled.giasin@port.ac.uk

J. Hawxwell
jacob.hawxwell@sandvik.com

J. Sinke
j.sinke@tudelft.nl

H. Dhakal
hom.dhakal@port.ac.uk

U. Köklü
ugurkoklu@gmail.com

E. Brousseau
brousseaue@cardiff.ac.uk

[1] Advanced Materials and Manufacturing (AMM) Research Group, School of Mechanical and Design Engineering, University of Portsmouth, Portsmouth PO1 3DJ, UK

[2] Sandvik Coromant, Unit 8, Morse Way, Waverley, Sheffield S60 5BJ, UK

[3] Delft University, Kluyverweg 1, 2629 HS Delft, Netherlands

[4] Department of Mechanical Engineering, Faculty of Engineering, Karamanoglu Mehmetbey University, 70100 Karaman, Turkey

[5] School of Engineering, Cardiff University, Cardiff CF24 3AA, UK

Table 1 Previous drilling studies reporting on hole size, circularity, perpendicularity, and cylindricity when drilling different aeronautical materials [2]

Workpiece material	Hole size (mm)	Circularity (μm)	Perpendicularity (mm)	Cylindricity (mm)	Reference
GLARE® 2B	5.96–6.022	4–34	0.004–0.028	–	[3, 4]
GLARE® 3 GLARE® 5	6.25–6.375	–	–	–	[26]
GLARE® 6 GLARE®3	5.013–5.063	–	–	–	[41]
GFRP	–	4–41	–	–	[43]
GFRP	–	42.5–312	–	–	[44]
CFRP	5.02–5.95	80–250	–	–	[45]
CFRP	–	–	–	0.025–0.091	[46]
CFRP/Al2024	–	6–25	–	–	[47]
Al2024-T3	–	4–33	–	–	[47]
Al2024-T3	6.007–6.040	6–39	–	–	[25]
Al6061	–	19–182	–	–	[48]

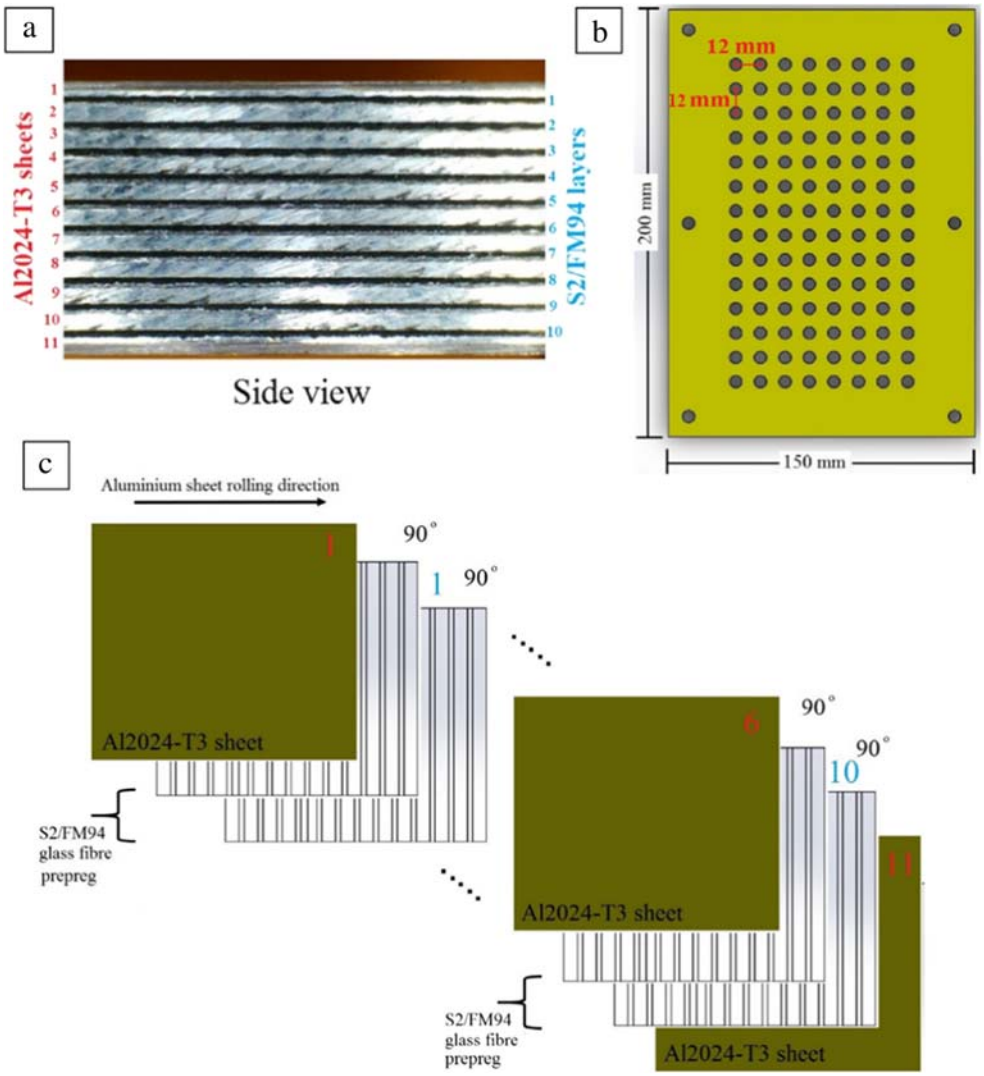

Fig. 1 Details of the GLARE® workpiece used in the current study. **a** Side view. **b** Front view. **c** Laminate configuration [3, 50]

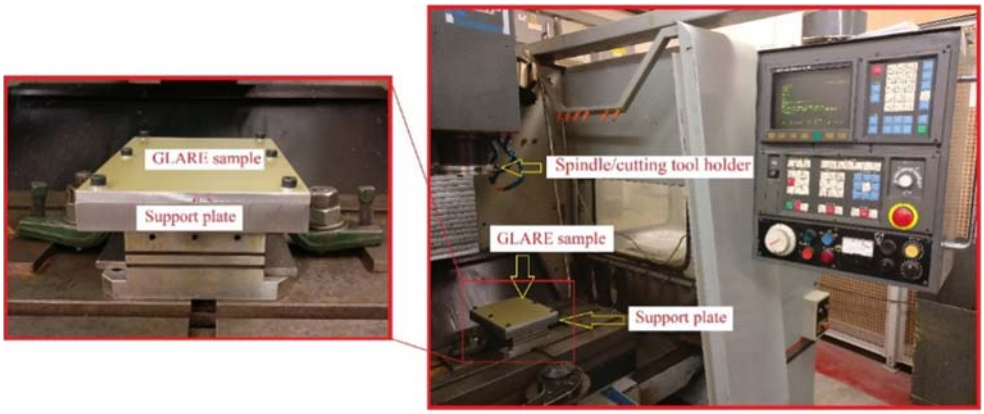

Fig. 2 Setup of the GLARE® laminate inside the CNC machine [49]

tolerances depending on their final application, customer specification or current standards. Hole size, circularity, cylindricity and perpendicularity error are some of the most inspected hole quality parameters in aerospace applications.

Fibre metal laminates (FMLs) are made from thin layers of composites materials and sheets of metallic alloys bonded together using adhesive epoxies [8–11]. The metallic sheets are usually made from aluminium alloys, while the composite layers are usually made from glass (GLARE®), aramid (ARALL®) or carbon fibres (CARALL®) [11]. The typical thickness of the metallic sheets can be anything between 0.25 and 0.5 mm, and the total material thickness is typically less than 1 mm but can be as thick as 20 mm [9, 12, 13]. GLARE® offers weight savings between 15 and 30% and improved fatigue resistance over standard aeronautical aluminium alloys [10, 14, 15]. The first utilisation of GLARE® panels was in the Boeing 737, 757 and 777 cargo floors and liners, in the Learjet 45 and on the C-17 Globemaster III cargo doors [8, 11, 16–19]. Currently, GLARE® is installed in parts of the Airbus A380 fuselage skin, lateral shells and the vertical stabiliser [9, 20, 21].

Table 2 General information about the drill bits used and their coatings [49]

Description	Drill A	Drill B	Drill C
Drill material	Tungsten carbide		
Drill diameter (mm)	6		
Helix angle (°)	30		
Point angle (°)	140		
Tolerance	M7		
Coating	TiAlN	TiN	AlTiN/TiAlN
Colour	Violet black	Gold	Black
Coating thickness (μm)	1.5–4	1.5–3	1.5–5
Layer structure	Monolayer	Monolayer	Multilayer
Nanohardness (HV 0.05)	3300	2400	3800
Friction coefficient	0.5–0.55	0.5	0.6
Thermal stability (°C)	700–800	595	900

Drilling and milling operations are applied to GLARE® structures for assembly and riveting purposes [9, 21]. Experimental machining studies on GLARE® laminates have been increasing in the last 20 years [2, 4, 6, 9, 21–39]. Previous studies on drilling GLARE® studied the impact of machining parameters, drill geometry, workpiece thickness, fibre orientation and cooling strategy on several hole quality parameters [2–4, 6, 9, 21–40]. A smaller number of studies also investigated the influence of drill geometry and coating on the generated drilling forces and hole quality [4, 26, 40–42]. Reported findings suggest that carbide drills perform better than uncoated and high-speed steel drills due to the abrasive glass fibre layers [9, 21, 41]. Other studies investigated the influence of machining coolants [3, 9, 22, 23]. It was found that cryogenic and minimum quantity lubrication cooling technologies tended to reduce burrs, surface roughness and workpiece temperature when compared to dry conditions [3, 9, 22, 23]. The laminate thickness and fibre orientation were also found to impact the hole quality [6, 22, 23, 27].

In comparison with more traditional engineering materials, only a few studies looked into the impact of drilling parameters, drill coating and geometry on specific hole quality metrics, i.e. hole size, circularity and perpendicularity, when drilling FMLs [2–4, 22–24]. For these studies, the measured hole parameters and their values are summarised in Table 1. Also, this table reports such results for studies that focussed on the drilling of the constituent materials used in FMLs. Based on this body of literature, it can be said that none of the previous work on the hole

Table 3 Drilling parameters used in the study showing the structure of the design of experiments

	Machining levels		
Feed rate (f) (mm/min)	300	450	600
Spindle speed (n) (rpm)	3000	4500	6000
Drill coating	TiAlN	TiN	AlTiN/TiAlN

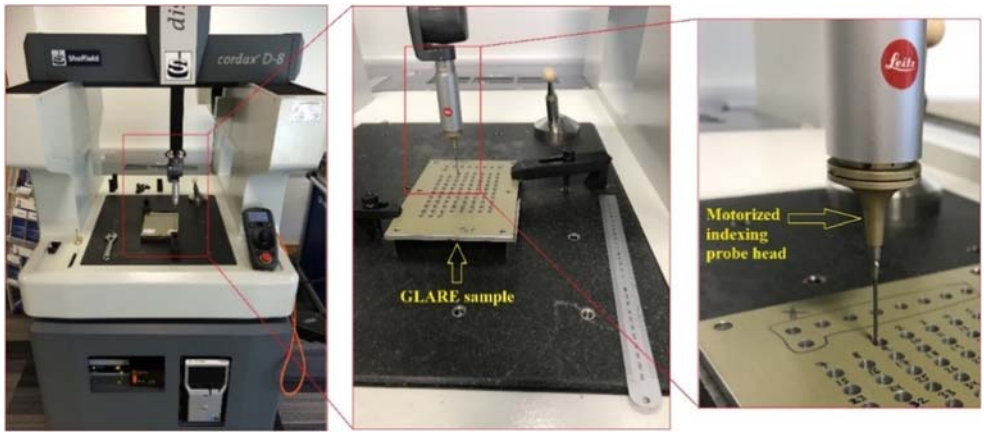

Fig. 3 Measurement of hole geometrical tolerances

drilling in FMLs investigated the impact of drill coating when the drill geometry is fixed (i.e. point angle, helix angle, diameter). For this reason, the work reported here investigates the impact of three drill coatings on hole quality parameters (hole size, circularity, cylindricity and perpendicularity) under different spindle speeds and feed rates while using same drill geometry (i.e. drill size, helix and angles). In this way, it is possible to evaluate specifically the influence of drill coating on hole quality. The analysis reported in this work is carried out using design of experiments (DoE) and ANOVA is implemented to study the impact of the feed rate, the spindle speed and their interactions on the studied outputs.

2 Materials and method

2.1 Workpiece details

The workpiece material utilised in this research is a GLARE® 2B laminate as shown in Fig. 1a. The laminate is made up of Al2024-T3 aluminium sheets and S2/FM94 glass fibre-epoxy layers [3, 4, 6]. The distance between the centres of two holes drilled adjacent to each other was kept constant as illustrated in Fig. 1b [49]. The workpiece dimensions were 200 mm × 150 mm and approximately 7.13 mm thick. Each glass fibre layer was made up of two plies oriented at 90°/90° with respect to the aluminium rolling direction (0°) as represented with Fig. 1c.

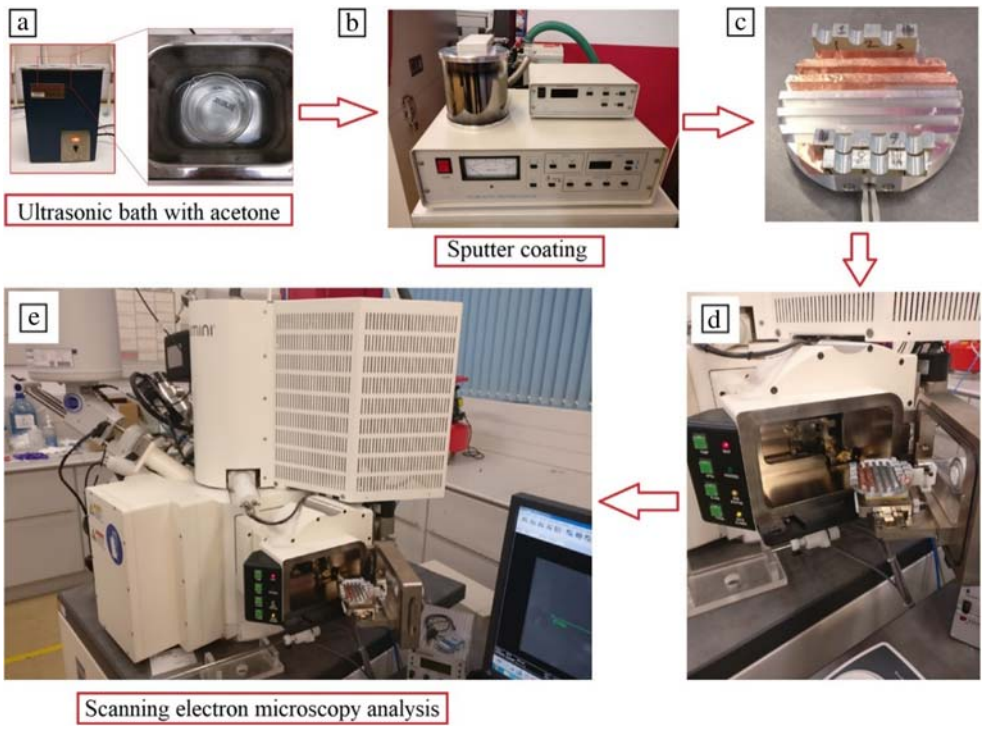

Fig. 4 Sample preparation for SEM analysis. **a** Ultrasonic bath with acetone. **b** Sputter coating. **c** Mounting base. **d** Interlock chamber. **e** Carl Zeiss 1540 XB SEM

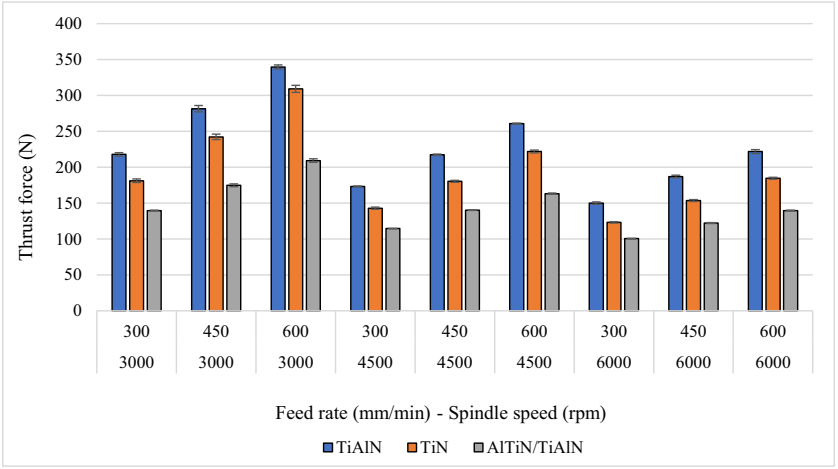

Fig. 5 Thrust force results for different types of drill coating

2.2 Machining setup and drill details

A Geo Kingsbury three-axis milling machine was used to drill the holes in the GLARE® workpiece [49]. The sample was placed on the top of a 20-mm-thick support plate made from stainless steel to restrict the movement or bending of the laminate similarly to previous studies [3, 4, 6, 22, 49]. The complete setup is shown in Fig. 2. The drilling tests were conducted without the use of any coolants (dry drilling). Additional drilling tests were conducted on a Quaser MV 154-C-CNC milling machine to measure the thrust force. The thrust force was measured using a KISTLER 9257B dynamometer. A DynoWare software, KISTLER 5697A data acquisition system and 5070A 8-channel charge amplifier were used for measurement and data acquisition.

The drilling tools were made from coated carbide material with a Ø6-mm nominal diameter. All drills had a fixed 140° point angle, and a 30° helix angle which was based on previous studies and literature [2–4, 6, 22–26, 41, 50]. The three types of coatings investigated in this work were TiAlN, TiN and AlTiN/TiAlN. The drills had an M7 tolerance which means that their actual diameter was between Ø6 mm + 0.004 mm and Ø6 mm + 0.016 mm. The full details of dimensions, geometry and other properties of the drills employed are given in Table 2.

2.3 Machining parameters and design of experiments

Three feed rates (f) and three spindle speeds (n) were used in the current study according to previous literature on drilling GLARE® laminates [3, 4, 6, 22, 23, 26, 27, 47, 51]. A design

Table 4 ANOVA results for thrust force

Thrust force						
Source	DF	Adj SS	Adj MS	F value	P value	Percentage contribution
Model	28	280,043	10,001.5	1614.99	0	99.89%
Blocks	2	31	15.3	2.48	0.094	0.01%
Linear	6	264,408	44,068	7115.84	0	94.31%
Spindle speed	2	87,987	43,993.4	7103.8	0	31.38%
Feed rate	2	83,151	41,575.7	6713.41	0	29.66%
Coating	2	93,270	46,634.9	7530.33	0	33.27%
2-Way interactions	12	15,055	1254.5	202.58	0	5.37%
Spindle speed × feed rate	4	5730	1432.5	231.32	0	2.04%
Spindle speed × coating	4	4669	1167.2	188.48	0	1.67%
Feed rate × coating	4	4655	1163.9	187.93	0	1.66%
3-Way interactions	8	550	68.8	11.11	0	0.20%
Spindle speed × feed rate × coating	8	550	68.8	11.11	0	0.20%
Error	52	322	6.2			0.11%
Total	80					100.00%

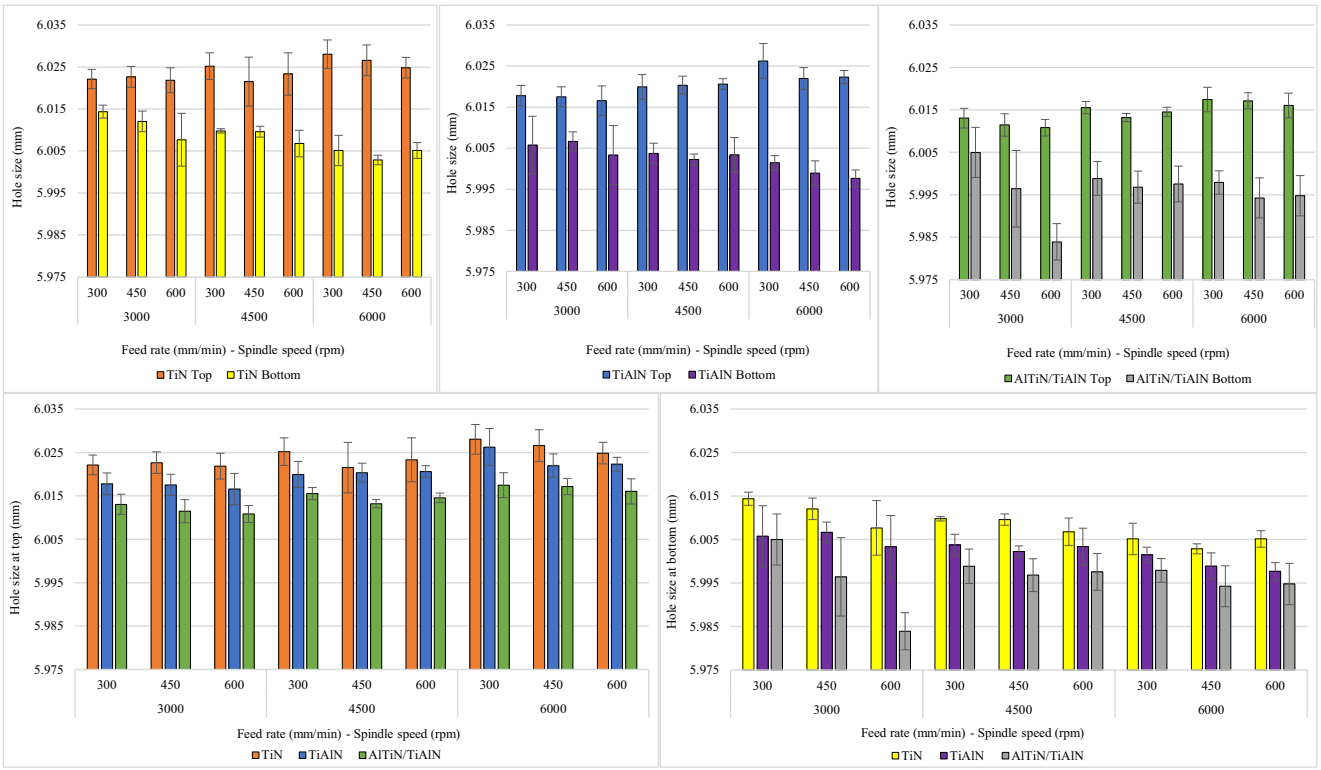

Fig. 6 Hole size for different types of coating at top and bottom location

of experiments (DoE) approach was implemented using a full factorial design composed of three levels and with a total of 27 runs (L_{27} orthogonal array). The proposed orthogonal array can determine the influence of the spindle speed, feed rate and drill coating and their linear interactions on the studied hole parameters. The analysis of variance (ANOVA) was carried out to determine the percentage contribution of the drilling parameters and drill coating on the studied hole quality parameters. Each trial was repeated three times resulting in drilling a total of 81 holes and the reported results represent the average of the three drilling tests. For each coating, each set of corresponding nine holes was drilled with a fresh drill to minimise any impact arising from drill wear [25]. A summary of the drilling parameters used in this study is provided in Table 3.

2.4 Measurement of hole geometrical tolerances

The hole geometrical tolerances (hole size, circularity, perpendicularity and cylindricity) were measured using a Sheffield Cordax-D8 Discovery III Coordinate Measurement Machine (CMM) [2–4]. The workpiece was clamped on the CMM table as shown in Fig. 3, and the measurements were taken at two locations at the top and the bottom of each hole (1 mm and 6 mm, respectively). A Leitz stylus equipped with a 2-mm ruby probe was employed to scan the borehole with an average of 30 contacts per mm at a scanning speed of 0.5 mm/s using an LSP-X1s probe head. The machine accuracy factory specification is 4.9 + 5 L/1000 μm; the maximum uncertainty reported in the calibration report of the machine was 0.97 μm. A Mitutoyo Crysta-Apex S776 CMM was used to measure a set of drills sizes before drilling. The MPE_E (maximum permissible error) of the CMM used to measure the sizes of the drills was 1.7 + 3 L/1000, while the MPE_E of the CMM is used to measure hole tolerances was 4.9 + 5 L/1000 μm. MPE_E follows the form of $MPE_E = A + L/K$, where A is a constant (μm) specified by the manufacturer, K is a dimensionless constant specified by the manufacturer and L is the measured length (mm) in this case is 6 mm. Therefore, the accuracies at which the CMM measures the distance between any two points up to a distance of 6 mm for the two CMM machines used in this study were 0.0349 μm and 0.0197 μm. The drill diameters for TiN-, TiAlN- and AlTiN/TiAlN-coated tools were found to be 6.0146 mm, 5.994 mm and 5.9965 mm, respectively.

2.5 Scanning electron microscopy

SEM was employed to inspect the machined hole surface for any drilling-induced damage. Each hole was cut in half and was then subjected to an ultrasonic bath to eliminate any unwanted debris from the borehole surface as shown in Fig. 4a. The sectioned holes were then sputter-coated before the inspection with the SEM (Fig. 4b). They were then secured on a platform using a copper double-sided tape before inspecting them as shown with Fig. 4 c and d. Magnifications (× 35–500)

and 10 keV voltage were applied to visualise the borehole walls as necessary.

3 Results and discussion

3.1 Thrust force analysis

Figure 5 shows the average thrust force from the three runs for each tool coating under different cutting parameters. It is noticeable that the TiAlN drills consistently produced the largest thrust force under all cutting parameters, followed by the TiN and AlTiN/TiAlN drills, respectively. It is also observed from this figure that increasing the feed rate increased the thrust force, while increasing the spindle speed decreased it, which is in agreement with previous studies on the drilling of GLARE® laminates [3, 6]. The thrust force recorded using TiAlN drills was between 9.87 and 21.86% higher than that recorded using TiN tools under the same cutting parameters. Similarly, the thrust force recorded using TiAlN drills was between 49.26 and 62.27% higher than that recorded using AlTiN/TiAlN tools.

A previous study also reported that the cutting forces generated using TiN-coated drills were lower than those generated by TiAlN-coated drills [52]. It could be speculated that the AlTiN/TiAlN coating provided a better self-lubricating effect due to its multilayer coating structure, but this needs to be confirmed in a future study. AlTiN/TiAlN tools combine two coatings in a micro-layered structure that is harder and more wear resistant than the two alone. As reported in Table 2, the TiAlN coating has an oxidation temperature of approximately 800 °C, a nano-hardness of 3300 (HV 0.05) and a friction coefficient of 0.5. The AlTiN/TiAlN coating, on the other hand, has an oxidation temperature of approximately 900 °C

Table 5 ANOVA results for hole size on the top and bottom regions

Source	DF	Adj SS	Adj MS	*F* value	*P* value	Percentage contribution
Hole size at the top						
Model	28	0.00181	6.5E−05	5.31	0	74.08
Blocks	2	5.6E−05	2.8E−05	2.31	0.109	2.28
Linear	6	0.00169	0.00028	23.13	0	69.17
Spindle speed	2	0.00037	0.00018	15.06	0	15.00
Feed rate	2	4.2E−05	2.1E−05	1.73	0.187	1.71
Coating	2	0.00128	0.00064	52.6	0	52.45
2-Way interactions	12	3.2E−05	3E−06	0.22	0.997	1.31
Spindle speed × feed rate	4	0.00002	5E−06	0.4	0.807	0.82
Spindle speed × coating	4	1.3E−05	3E−06	0.26	0.903	0.53
Feed rate × coating	4	0	0	0	1	0
3-Way interactions	8	3.1E−05	4E−06	0.32	0.955	1.27
Spindle speed × feed rate × coating	8	3.1E−05	4E−06	0.32	0.955	1.27
Error	52	0.00063	1.2E−05			25.91
Total	80	0.00245				100
Hole size at the bottom						
Model	28	0.00363	0.00013	7.05	0	79.17
Blocks	2	0.00042	0.00021	11.5	0	9.23
Linear	6	0.00249	0.00042	22.62	0	54.41
Spindle speed	2	0.00026	0.00013	7.1	0.002	5.69
Feed rate	2	0.00029	0.00015	7.92	0.001	6.35
Coating	2	0.00194	0.00097	52.83	0	42.36
2-Way interactions	12	0.0005	4.1E−05	2.26	0.022	10.86
Spindle speed × feed rate	4	0.00024	5.9E−05	3.21	0.02	5.15
Spindle speed × coating	4	0.00016	0.00004	2.15	0.087	3.45
Feed rate × coating	4	0.0001	2.6E−05	1.41	0.243	2.27
3-Way interactions	8	0.00021	2.7E−05	1.45	0.197	4.67
Spindle speed × feed rate × coating	8	0.00021	2.7E−05	1.45	0.197	4.67
Error	52	0.00096	1.8E−05			20.86
Total	80	0.00458				100.00

with a 0.6 friction coefficient. Although such coating's parameters are fairly close to those of TiAlN's, AlTiN/TiAlN still has the highest thermal stability between the two coatings thus providing exceptional oxidation resistance and extreme hardness when used in multilayer coating system and performing better in dry drilling.

The ANOVA analysis shown in Table 4 reveals that the cutting parameters and tool coating contributed somewhat equally towards the thrust force with each contributing around 30%. In addition, their linear interaction had some minor impact on the thrust force. This could indicate that a proper combination of cutting parameters and tool coating would result in reduced thrust force and drilling-induced damage in the glass fibre layers of the laminate.

3.2 Hole size analysis

Figure 6 shows the average hole size obtained when drilling the GLARE® sample under different drilling parameters and drill coatings for both the top and bottom regions of the hole. Overall, the hole size at the top ranged between 6.010 and 6.028 mm, while this range decreased between 5.98 and 6.014 mm at the bottom. Similar results were reported in previous studies in drilling GLARE® and Al2024 alloy [3, 22, 25, 53]. Oversized holes were produced at the top regardless of the type of drill coating or drilling parameters used. It should be noted that all drills were produced with a tolerance range of +4 μm to +16 μm. In addition, there was a significant variation in the drill diameters as shown previously in Sect. 2.4. For this reason, it is argued that no firm conclusion may be made from the direct observation of Fig. 6 in terms of which drill coating resulted in the largest hole oversize. Instead, one can use data in Fig. 6 to analyse the relative reduction in the hole diameter between the top and the bottom region for a given type of coating. The average reduction in hole size between the top and the bottom region was 15.86 μm, 17.78 μm and 18.19 μm for TiN-, TiAlN- and AlTiN/TiAlN-coated drills, respectively. Hole shrinkage is common when drilling composites due to the relaxation of the lamina [22, 54]. Therefore, the lower coefficient of friction of TiN-coated drills compared to the other two coatings might have caused a lower temperature at the cutting zone leading to reduced hole shrinkage with depth. If the actual drill size for each coating is considered when comparing the measured hole sizes obtained by the three coatings, then TiN-coated drills produced holes with least deviation from the drill original size followed by AlTiN/TiAlN and TiAlN coatings, respectively. However, this requires further investigation which will be carried out in a future study.

The largest hole deviation from the nominal value on the top region took place when drilling at the highest spindle speed, i.e. n=6000 rpm, with the lowest feed rate, i.e. f=300 mm/min. This may be due to increased drill vibration at higher spindle speed values [55]. On the contrary, the smallest hole deviation at the top occurred when drilling at the lowest spindle speed, i.e. n=3000 rpm, and with the

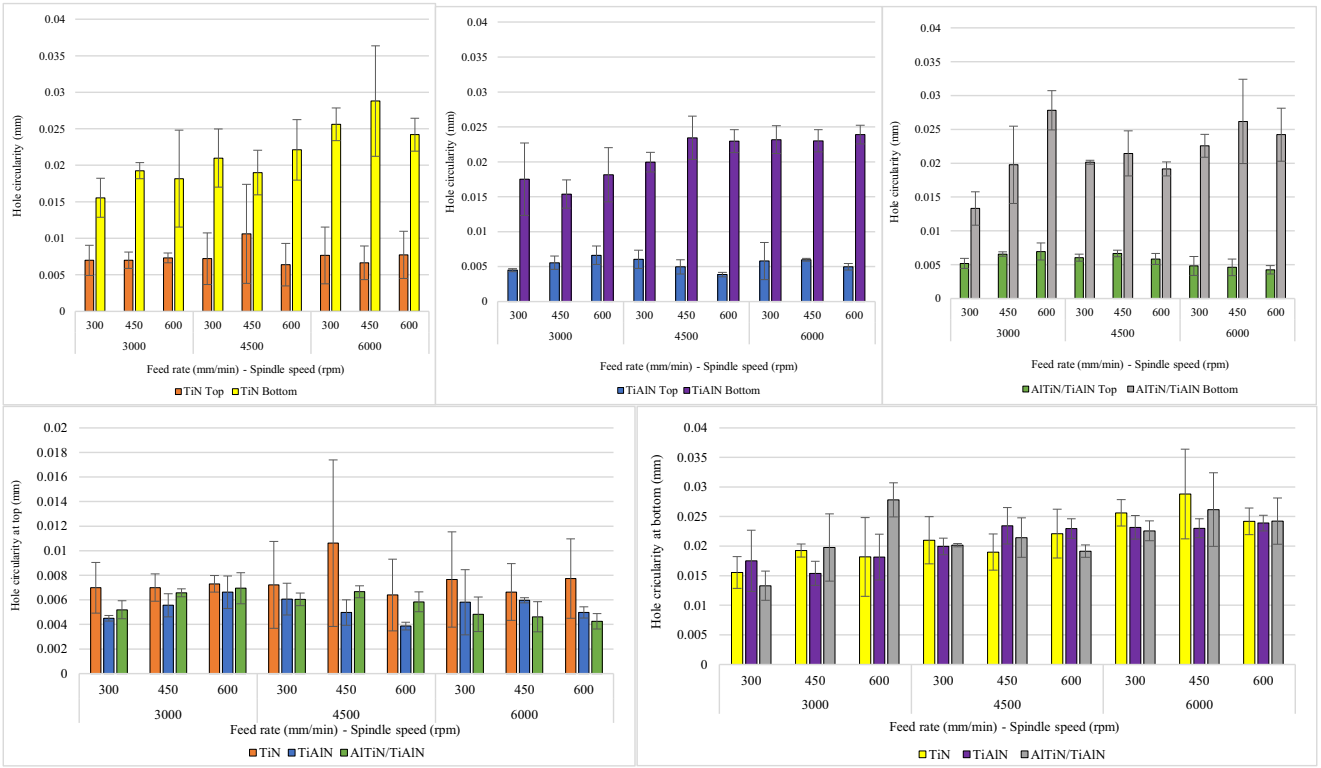

Fig. 7 Hole circularity for different types of coating at top and bottom

highest feed rate, f=600 mm/min, except for the drills with TiN coating where the smallest deviation was achieved at n=4500 rpm and f=450 mm/min. On the bottom region, the largest hole deviation from the nominal value occurred for a different set of drilling conditions for each of the drill coating. This may indicate that the impact of drill coating on hole size becomes more significant with the increase in hole depth.

From the data presented in Fig. 6, it can also be said that, generally, the hole size on the top increased with the increase of spindle speed and decreased on the bottom surface with the increase of the spindle speed when drilling at constant feed rate. Thus, different phenomena, related to the increase in spindle speed, occur at the entrance and exit of the holes. For the bottom region, the continuous rubbing of the drill and evacuated hot chips increase the temperature at the cutting zone leading to thermal shrinkage [56]. This does not happen at the top surface as the more dominant influence in this region is the drill vibration. Finally, it can also be noted that drilling at the following combinations of feed rates and spindle speeds of 300/3000, 450/4500 and 600/6000 ((mm/min)/rpm) showed that hole size at top tended to increase, while at the bottom, it tended to decrease with the reduction of drilling time.

The ANOVA analysis provided in Table 5 shows that the parameters drill coating and spindle speed had a significant impact on hole size on the top region with 52.4% and 15.0% contribution, respectively. For the bottom region, the ANOVA results imply that all three input parameters had a significant impact on hole size. However, the dominant contribution came from the parameter drill coating with 42.4%, thus confirming an earlier comment made when discussing the results of Fig. 6.

Ideally, holes drilled in aeronautical structures should be close to their required nominal diameter for optimum rivet joint performance [3]. Having an oversized or undersized hole

Table 6 ANOVA results for hole circularity

Source	DF	Adj SS	Adj MS	F value	P value	Percentage contribution
Circularity on the top						
Model	28	0.000219	0.000008	1.35	0.175	41.95
Blocks	2	0.000069	0.000035	5.93	0.005	13.21
Linear	6	0.000082	0.000014	2.35	0.044	15.70
Spindle speed	2	0.000005	0.000003	0.44	0.649	0.96
Feed rate	2	0.000005	0.000002	0.39	0.681	0.96
Coating	2	0.000072	0.000036	6.21	0.004	13.79
2-Way interactions	12	0.000045	0.000004	0.64	0.799	8.62
Spindle speed × feed rate	4	0.000024	0.000006	1.04	0.396	4.59
Spindle speed × coating	4	0.000018	0.000005	0.78	0.546	3.44
Feed rate × coating	4	0.000002	0.000001	0.1	0.981	0.38
3-Way interactions	8	0.000024	0.000003	0.51	0.843	4.59
Spindle speed × feed rate × coating	8	0.000024	0.000003	0.51	0.843	4.59
Error	52	0.000303	0.000006			58.04
Total	80	0.000522				100
Circularity on the bottom						
Model	28	0.001361	0.000049	3.24	0	63.56
Blocks	2	0.000261	0.00013	8.69	0.001	12.19
Linear	6	0.000639	0.000107	7.1	0	29.85
Spindle speed	2	0.00054	0.00027	18	0	25.22
Feed rate	2	0.000089	0.000045	2.97	0.06	4.16
Coating	2	0.00001	0.000005	0.33	0.719	0.47
2-Way interactions	12	0.000258	0.000021	1.43	0.182	12.05
Spindle speed × feed rate	4	0.000101	0.000025	1.68	0.169	4.72
Spindle speed × coating	4	0.000099	0.000025	1.66	0.174	4.62
Feed rate × coating	4	0.000058	0.000014	0.96	0.438	2.71
3-Way interactions	8	0.000203	0.000025	1.69	0.123	9.48
Spindle speed × feed rate × coating	8	0.000203	0.000025	1.69	0.123	9.48
Error	52	0.00078	0.000015			36.43
Total	80	0.002141				100

would imply additional post-machining operations such as reaming process to achieve desired hole size. In the current study, the variation of hole size did not exceed the interval [−16.0 μm + 26.2 μm] which is within the upper range of H9 (0 to + 30 μm) hole tolerance recommended by aerospace manufacturers [3, 57]. Besides, industrial reports of drill manufacturers indicate that hole tolerances in aeronautical materials including GLARE® could vary between ± 20 and ± 40 μm [3, 58]. This means that hole sizes obtained in this study are within the allowable range and would only require a reaming process to enlarge the undersized holes.

3.3 Hole circularity analysis

Figure 7 shows the average hole circularity in the GLARE® sample under different drilling parameters and drill coatings at the top and bottom regions. Overall, the average hole circularity on the top was better as it ranged between 3.08 and 10.6 μm, while at the bottom, it was between 13.3 and 28.8 μm. The results are in line with circularity data reported in previous studies on drilling same grade and thickness of GLARE® laminates, particularly the fact that hole circularity is likely to worsen with depth due to the gradual increase in thermal load while cutting through the material and the non-isotropic nature of the coefficient of thermal expansion of the glass fibre layers [3, 22, 25]. However, this observation disagrees with previous studies on drilling metals which report that the deviation from circularity at the hole inlet is worse than that at the hole outlet due to the dynamic instability of the drill during its initial contact with the workpiece. The better values observed at the outlet in holes drilled in metallic materials were reportedly due to self-pointing guidance action of the hole to the drill with increasing depth [59–61]. Other studies on drilling aluminium alloys reported that there are highly non-linear variations in hole circularity throughout the depth of the hole due to the presence of other factors such as fixture/machine drill vibration/drill deflections and damping characteristics [25, 53]. In addition, there was a significant variation in the drill diameters as shown previously in Sect. 2.4. For this reason, it is argued that no firm conclusion may be made from the direct observation of Fig. 7 in terms of which drill coating resulted in the least hole circularity. Instead, one can use data in Fig. 7 to analyse the relative difference in the hole circularity between the top and the bottom region for a given type of

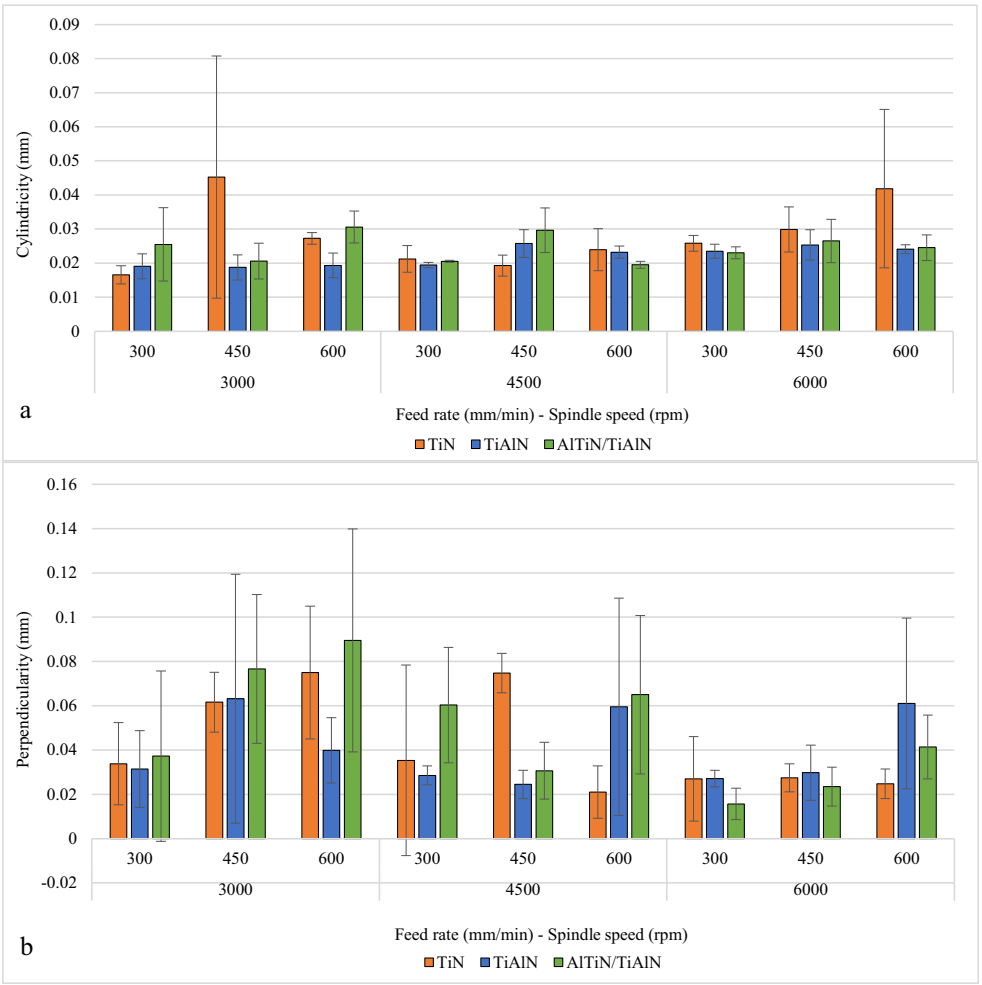

Fig. 8 Hole. **a** Cylindricity. **b** Perpendicularity

coating. The variation in repetitions was significant at the bottom which could be due to the weakening of the hole structure with the reduction in material thickness to be removed from the hole as the drill progresses towards the exit side of the hole. It is also speculated that there might be some other factors affecting those holes tolerances such as the location of the hole and the clamping technique. Such factors will be considered for investigation in future studies.

When considering all the experimental data, the worst hole circularity on the top region occurred when drilling at n=4500 rpm, f=450 mm/min using TiN coating, while the best hole circularity was achieved when drilling at n=4500 rpm, f=600 mm/min using TiAlN coating. Generally, for TiN-coated drills, hole circularity at the top region deteriorated with the increase of the spindle speed. For both TiAlN- and AlTiN/TiAlN-coated drills, hole circularity on the top region became better with the increase in spindle speed except for the lowest feed rate value considered.

Regarding the circularity of holes on the bottom region, for TiN coating, it tended to worsen with the increase of the spindle speed at all feed rates. For AlTiN/TiAlN coating, the hole circularity at the bottom tended to worsen with the increase of the feed rate when drilling at n= 3000 rpm, while it tended to worsen then become better with the increase of the feed rate when drilling at spindle speeds of n= 4500 and n= 6000 rpm. Drilling at feed rate/spindle speed ratios of 0.1 (0.1 mm/rev) showed that hole circularity at the top tended to be worst when drilling at of n= 4500 and f= 450 mm/min. However, at the bottom, the hole circularity tended to worsen with the reduction of drilling time which indicates that drilling at faster rates will be on the expense of worsening hole circularity.

The ANOVA analysis provided in Table 6 shows that only the drill coating had a major impact on hole circularity for the

Table 7 ANOVA results for hole cylindricity and Perpendicularity

Source	DF	Adj SS	Adj MS	*F* value	*P* value	Percentage contribution
Hole cylindricity						
Model	28	0.00574	0.00021	12.59	0	87.14
Blocks	2	0.00528	0.00264	162.15	0	80.15
Linear	6	0.00014	2.3E−05	1.42	0.225	2.112
Spindle speed	2	1.2E−05	6E−06	0.37	0.692	0.182
Feed rate	2	0	0	0	0.999	0
Coating	2	0.00013	6.3E−05	3.89	0.027	1.929
2-Way interactions	12	0.00021	1.8E−05	1.09	0.391	3.221
Spindle speed × feed rate	4	7.8E−05	1.9E−05	1.2	0.323	1.185
Spindle speed × coating	4	0.00011	2.8E−05	1.72	0.161	1.701
Feed rate × coating	4	2.2E−05	6E−06	0.34	0.848	0.334
3-Way interactions	8	0.00011	1.4E−05	0.84	0.574	1.656
Spindle speed × feed rate × coating	8	0.00011	1.4E−05	0.84	0.574	1.656
Error	52	0.00085	1.6E−05			12.85
Total	80	0.00658				100
Hole perpendicularity						
Model	28	0.001361	0.000049	3.24	0	63.56
Blocks	2	0.000261	0.00013	8.69	0.001	12.19
Linear	6	0.000639	0.000107	7.1	0	29.84
Spindle speed	2	0.00054	0.00027	18	0	25.22
Feed rate	2	0.000089	0.000045	2.97	0.06	4.15
Coating	2	0.00001	0.000005	0.33	0.719	0.467
2-Way interactions	12	0.000258	0.000021	1.43	0.182	12.05
Spindle speed × feed rate	4	0.000101	0.000025	1.68	0.169	4.71
Spindle speed × coating	4	0.000099	0.000025	1.66	0.174	4.62
Feed rate × coating	4	0.000058	0.000014	0.96	0.438	2.7
3-Way interactions	8	0.000203	0.000025	1.69	0.123	9.48
Spindle speed × feed rate × coating	8	0.000203	0.000025	1.69	0.123	9.48
Error	52	0.00078	0.000015			36.43
Total	80	0.002141				100

top surface while it was only the spindle speed which was identified as the significant contributor for the bottom surface, with 13.79% and 25.22%, respectively. This is somewhat different from previous studies which showed that the spindle speed and the feed rate had a significant effect on hole circularity on both surfaces with a higher contribution by the spindle speed [2, 6]. This is because the current study also considered drill coating as one of the input parameters. Also, this may be due to the presence of non-linear trend in the model, as indicated by the large error present in the model, i.e. from 36.43 to 58.04%.

3.4 Hole cylindricity and perpendicularity

Figure 8 shows the average values of hole cylindricity and perpendicularity under different drilling parameters for the three types of drill coatings used. The average hole cylindricity ranged between 16.5 and 45.2 μm as shown in Fig. 8a. The worse hole cylindricity occurred using TiN coating when drilling at a spindle speed of n= 3000 rpm and a feed rate of f= 450 mm/min. The best hole cylindricity occurred using TiN coating when drilling at a spindle speed of n= 3000 rpm and a feed rate of f= 300 mm/min. Hole cylindricity tended to worsen with the increase of the feed rate when drilling at spindle speeds of n= 4500 and 6000 rpm using TiN-coated drills. For TiAlN- and AlTiN/TiAlN-coated drills, hole cylindricity tended to deteriorate and then improve with the increase of feed rate at spindle speeds of n= 4500 and 6000 rpm.

Hole perpendicularity became worse with the increase of the feed rate when drilling at a spindle speed of n=3000 rpm for TiN and AlTiN/TiAlN coatings. A similar trend is observed with the increase of the feed rate when drilling at a spindle speed of n=6000 rpm for TiAlN and AlTiN/TiAlN coatings, which could be due to the increase in feed force and vibrations with the increase of the feed rate [4]. The average hole perpendicularity ranged from 0.015 to 0.089 mm; the highest and lowest perpendicularity was found to occur when drilling using AlTiN/TiAlN coating at n= 6000 rpm and f= 300 mm/min and n= 3000 rpm and f= 600 mm/min, respectively.

It is also worth to mention that the poor repeatability in hole perpendicularity data suggest that other input factors/parameters might have had an influence on hole perpendicularity which were not investigated in the current study [4]. One of the suggested factors is the location of the hole within the workpiece and the clamping setup of the laminate inside the CNC machine which will be investigated in a future study. In addition, the large errors in hole cylindricity and perpendicularity are common when measured for drilled holes in GLARE laminates as reported by previous studies [2, 3].

The R^2 (coefficient of determination) obtained from ANOVA analysis is low as shown in Table 7. Thus, the ANOVA analysis might not be suitable here to judge the impact of drilling parameters and drill coating on hole perpendicularity. ANOVA results show that the drill coating was the only contributing parameter on hole cylindricity, while the spindle speed was the only contributing factor on hole perpendicularity.

3.5 Scanning electron microscopy analysis

SEM images reported with Figs. 9 and 10 reveal that minor metal chipping, interlayer burrs, broken fibres and deformation marks on the surface of aluminium sheets can be observed due to contact with the drill. The types of damage resemble those observed in previously reported studies on drilling GLARE® under dry conditions [2, 3, 50]. The SEM inspection showed that the damage on the hole surface increased with hole depth. Smearing (plastic deformation) and other forms of deformation marks were observed on the surfaces of aluminium sheets which seemed to occur more frequently at higher feed rates which is in line with observations reported in a previous study [50]. Those deformation marks shown in Figs. 9 and 10 may be due to two distinct contact scenarios. The first type of deformation marks is speculated to be caused by the rubbing action of the metallic chips colliding with the hole walls while they are leaving the workpiece as shown in Fig. 9. In this case, the marks are helical in shape which

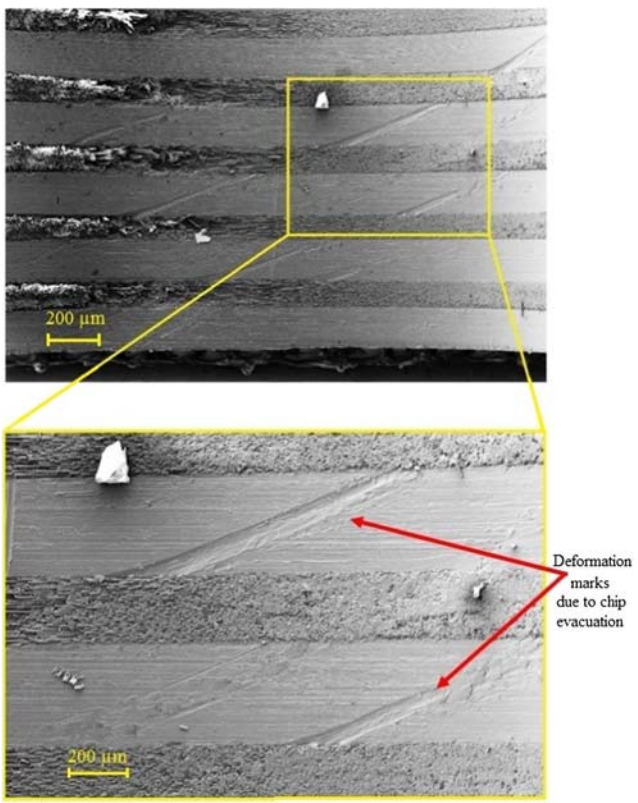

Fig. 9 SEM image of a borehole wall at f = 300 mm/min and n = 3000 rpm using a TiN-coated drill

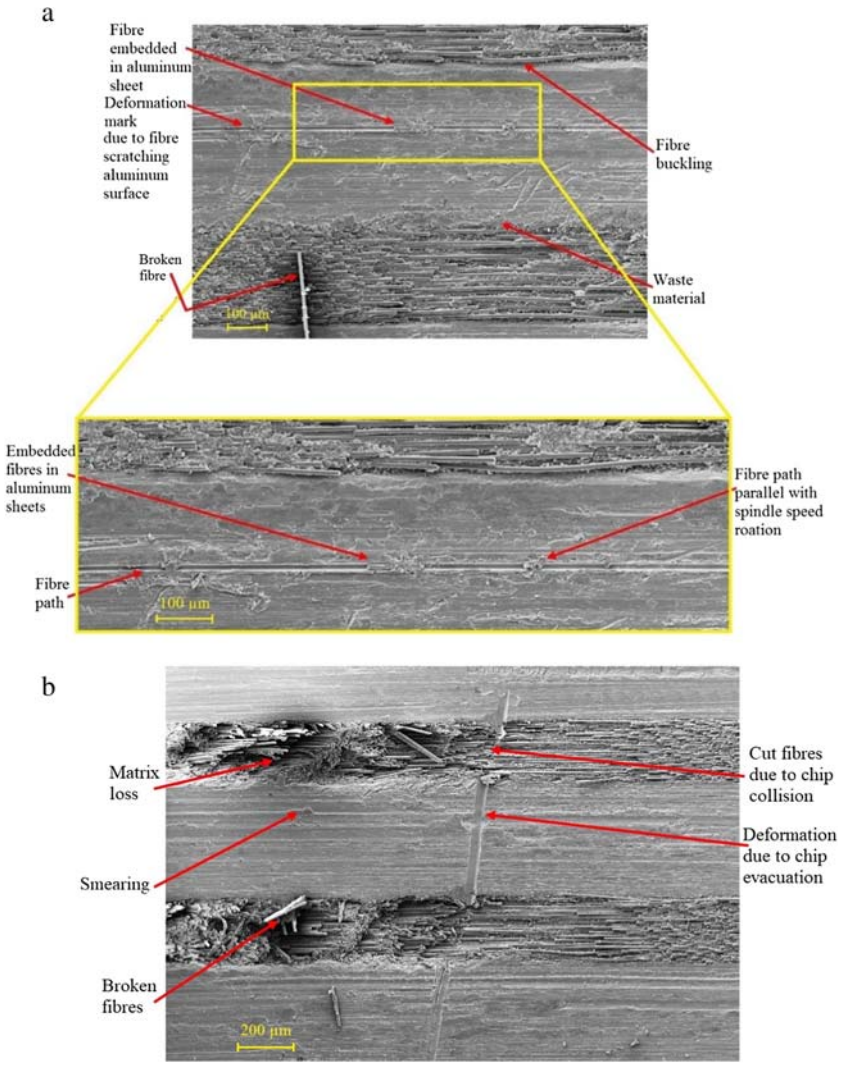

Fig. 10 SEM image of a borehole wall at **a** $f = 300$ mm/min and $n = 4500$ rpm using a AlTiN/TiAlN-coated drill **b** at $f = 300$ mm/min and $n = 6000$ rpm for TiAlN-coated drill

resembles the profile of the flute of the twist drill and is of several millimetres in length. This type of deformation marks could be also caused by the fierce rubbing on the hole walls due to vibrations and loss of drill eccentricity while it cuts through the material.

The second type of deformation marks is speculated to be caused by broken fibres which are trapped between the drill and borehole surface, causing them to be stressed onto the aluminium sheets and plastically deform their outer surface. In this case, the deformation marks appear to be parallel to the fibres as shown in Fig. 10a. Multiple instances of this type of marks were observed on the aluminium sheet. Some of the aluminium chips and broken glass fibres are not evacuated through the drill flutes and are eventually stressed into the edges of the aluminium sheets or into the voids formed in the glass fibre layers due to fibre pull-outs [50] as shown in Fig. 10b.

Interlayer burrs were observed around the borehole and through its thickness which might have caused further erosion in the glass fibre layers. Besides, the erosion in glass fibre layers might have been caused by the evacuated metallic chips [3, 50]. Powdery glass fibre chips and broken metallic chips were stressed into the laminate layers forming what is known as waste material as shown in Fig. 11a. The waste material—whether metallic or composite—is caused by the subsequent removal and adherent of laminate constituent materials debris during the drilling process [3]. The damage in borehole surface increased with the increase of both cutting parameters similar to previously reported studies [3, 50]. The results also showed that the edge of the last aluminium sheet is likely to be more deteriorated than the first aluminium sheet as reported in Fig. 11b. This could be attributed to the increased contact area between the drill and workpiece leading to higher frictional heat and plastic deformation. Therefore, burr formations tend to be higher at the bottom of the laminate than at the top as reported in previous literature [2, 3, 50]. The burrs formed at the entry of the hole were uniform around its edge, while burrs formed at the exit had an irregular appearance and heights.

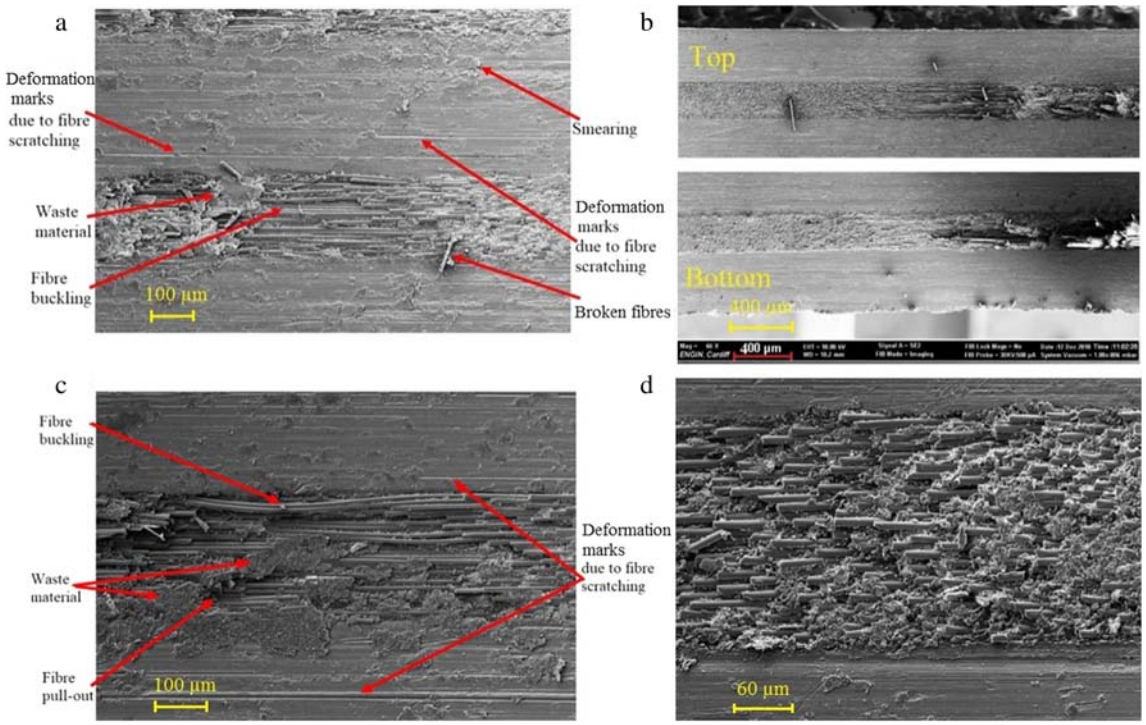

Fig. 11 SEM image of a borehole wall at **a** $f = 300$ mm/min and $n = 3000$ rpm using a AlTiN/TiAlN-coated drill. **b** The upper and lower aluminium sheets edges at $f = 300$ mm/min and $n = 3000$ rpm using a TiN-coated drill. **c** $f = 300$ mm/min and $n = 3000$ rpm using a AlTiN/TiAlN-coated drill **d** showing fibres with different uncut lengths at $f = 450$ mm/min and $n = 3000$ rpm using a TiN-coated drill

Delamination (type I) was present in the machined holes which takes place due to the progression of the drill into the laminate causing the peeled layers to bend either permanently due to plastic deformation or temporarily like a cantilever beam [3, 62]. A type II fibre buckling is seen in Fig. 11c due to compressive loading acting along their direction. Some chunks of fibres end with varying lengths were pointing out due to cutting by fracture as shown in Fig. 11d [3, 50, 62].

The SEM images did not show any signs of ply separation in composite layers or de-bonding between the laminate constituents. It is speculated that the sandwiched glass fibre layers between two metallic sheets from the top and bottom mimic the effect of support plates placed on the top or the bottom of a composite sample to reduce delamination, especially when drilling at higher feed rates [3, 63].

4 Conclusions

The machinability of GLARE® fibre metal laminates was investigated using twist drills to analyse the hole size, circularity, cylindricity and perpendicularity. The objective was to study the influence of drilling and three types of drill coatings (TiAlN, TiN and AlTiN/TiAlN) on the stated hole quality parameters. The influence of drill coatings had been previously studied in different GLARE® grades to evaluate the hole quality, but no study was previously carried out using the same drill geometry. The influence of drill coatings is a crucial factor in drilling aeronautical multimaterials made from composites and metals since they can prolong drill life and improve surface finish. However, only a handful number of researches had been conducted on drilling of GLARE® laminates in general and the influence of drill coating in particular. The following conclusions can be drawn from the study:

- The thrust force generated using AlTiN/TiAlN multilayer-coated drills was the lowest among the three coatings tested, followed by TiN and TiAlN coatings, respectively.
- The average reduction in hole size between the top and the bottom region was 15.86 µm, 17.78 µm and 18.19 µm for TiN-, TiAlN- and AlTiN/TiAlN-coated drills, respectively.
- Hole circularity at the bottom was worse than that at the top regardless of drill coating or drilling parameters. TiN-coated drills produced worst hole circularity at the top among the three coatings.
- Hole cylindricity was worst when using AlTiN/TiAlN- and TiN-coated drills; whole hole perpendicularity worsened with the increase of the feed rate.
- The ANOVA results showed that the spindle speed and drill coating had a significant influence on hole size and circularity, while drill coating was the only contributing parameter on hole cylindricity, and spindle speed was the only contributing factor on hole perpendicularity.

- SEM inspection showed that the damage generated on the walls of the hole are strongly influenced by the drilling parameters but not the drill coating. Fibre buckling, smearing, interlayer burr formation and deformation marks due to evacuated metallic chips and broken glass fibres were observed from the SEM images.

Acknowledgements The authors would like to thank Dr. Peter J. Kortbeek from DELFT University and the Fibre-Metal Laminate Centre of Competence (FMLC) for the provision of GLARE® sample. The authors would like to thank Dr. Carlton Byrne and Miss Gabriella Gorey from Cardiff University for assistance with the drilling tests.

Funding information The authors received support from the European Regional Development Fund through the Welsh Government for ASTUTE 2020 (Advanced Sustainable Manufacturing Technologies) to facilitate this work.

Data availability The raw data required to reproduce these findings are available upon request.

Open Access This article is licensed under a Creative Commons Attribution 4.0 International License, which permits use, sharing, adaptation, distribution and reproduction in any medium or format, as long as you give appropriate credit to the original author(s) and the source, provide a link to the Creative Commons licence, and indicate if changes were made. The images or other third party material in this article are included in the article's Creative Commons licence, unless indicated otherwise in a credit line to the material. If material is not included in the article's Creative Commons licence and your intended use is not permitted by statutory regulation or exceeds the permitted use, you will need to obtain permission directly from the copyright holder. To view a copy of this licence, visit http://creativecommons.org/licenses/by/4.0/.

References

1. Mouritz, A., *Introduction to aerospace materials*. 2012: Elsevier
2. Giasin K, Ayvar-Soberanis S (2017) An investigation of burrs, chip formation, hole size, circularity and delamination during drilling operation of GLARE using ANOVA. Compos Struct 159:745–760
3. Giasin K. (2017) *Machining Fibre Metal Laminates and Al2024-T3 aluminium alloy*. University of Sheffield
4. Giasin K (2018) The effect of drilling parameters, cooling technology, and fiber orientation on hole perpendicularity error in fiber metal laminates. The International Journal of Advanced Manufacturing Technology
5. Hocheng, H., *Machining technology for composite materials : principles and practice*. 2012, Cambridge, UK; Philadelphia, PA: Woodhead Pub
6. Giasin K, Ayvar-Soberanis S, Hodzic A (2015) An experimental study on drilling of unidirectional GLARE fibre metal laminates. Compos Struct 133:794–808
7. Campbell Jr, F.C. (2011) *Manufacturing technology for aerospace structural materials*. Elsevier
8. Vlot A (2001) *Glare: history of the development of a new aircraft material*. Springer Science & Business Media
9. Vlot A and Gunnink JW (2001) *Fibre metal laminates: an introduction*. Springer
10. Gunnink J, Vlot A, Alderliesten R, van der Hoeven W, Boer A. de, Sinke J, Ypma M, de Vries T, and Wittenberg T (2000) *Towards technology readiness of fibre metal laminates*. in *International Congress of Aeronautical Sciences, 22 nd, Harrogate, United Kingdom*
11. Vlot A, Vogelesang L, De Vries T (1999) Towards application of fibre metal laminates in large aircraft. Aircr Eng Aerosp Technol 71(6):558–570
12. De Graaf R, Meijer J (2000) Laser cutting of metal laminates: analysis and experimental validation. J Mater Process Technol 103(1): 23–28
13. Geert HJJ. Roebroeks PAH, Kroon EJ, Heinimann MB (2007) The development of central. In First International Conference on Damage Tolerance of Aircraft Structures (eds) Benedictus JSR, Alderliesten RC, Homan JJ. TU Delft, Delft
14. Elhajjar R, La Saponara V, and Muliana A (2013) *Smart composites: mechanics and design*. CRC Press
15. Seo H (2008) *Damage tolerance and durability of GLARE laminates*. ProQuest
16. Chawla KK (2012) *Composite materials: science and engineering*. Springer Science & Business Media
17. Baker AA, Rose LF, and Jones R (2003) *Advances in the bonded composite repair of metallic aircraft structure*. Vol. 1. : Elsevier
18. Alderliesten R (2009) On the development of hybrid material concepts for aircraft structures. Recent Patents on Engineering 3(1):25–38
19. Silberschmidt VV (2016) *Dynamic deformation, damage and fracture in composite materials and structures*. Woodhead Publishing
20. Pora J (2001) *Composite materials in the airbus A380–from history to future.* Proceedings of ICCM13, Plenary lecture, CD-ROM
21. Sinke J (2003) Manufacturing of GLARE parts and structures. Appl Compos Mater 10(4–5):293–305
22. Giasin K, Ayvar-Soberanis S, Hodzic A (2016) The effects of minimum quantity lubrication and cryogenic liquid nitrogen cooling on drilled hole quality in GLARE fibre metal laminates. Mater Des 89: 996–1006
23. Giasin K, Ayvar-Soberanis S, Hodzic A (2016) Evaluation of cryogenic cooling and minimum quantity lubrication effects on machining GLARE laminates using design of experiments. J Clean Prod 135:533–548
24. Giasin K, Ayvar-Soberanis S, French T, Phadnis V (2016) *3D Finite element modelling of cutting forces in drilling fibre metal laminates and experimental hole quality analysis*. Appl Compos Mater:1–25
25. Giasin K, Hodzic A, Phadnis V, Ayvar-Soberanis S (2016) Assessment of cutting forces and hole quality in drilling Al2024 aluminium alloy: experimental and finite element study. Int J Adv Manuf Technol 87(5–8):2041–2061
26. Pawar OA, Gaikhe YS, Tewari A, Sundaram R, Joshi SS (2015) Analysis of hole quality in drilling GLARE fiber metal laminates. Compos Struct 123:350–365
27. Tyczynski P, Lemanczyk J, Ostrowski R (2014) Drilling of CFRP, GFRP, glare type composites. Aircr Eng Aerosp Technol 86(4): 312–322
28. Paul S, Hoogstrate A, Van Praag R (2002) Abrasive water jet machining of glass fibre metal laminates. Proc Inst Mech Eng B J Eng Manuf 216(11):1459–1469
29. Praag RV (1996) *Hand drilling fiber metal laminates, guideline for successful hand drilling*. Fiber metal laminates, Handbook of workshop properties, Delft University of Science & Technology, Structures & Materials Laboratory, Delft University of Science & Technology. 9
30. Praag RV (1996) *Milling fiber metal laminate, tool wear tests, edge quality and justification of WP 3-200 to WP 3-250*. Fiber metal laminates, Handbook of workshop properties, Delft University of Science & Technology, Structures & Materials Laboratory. Delft University of Science & Technology. 19
31. van Praag, R. and J. Sinke, *Manufacturing fibre-metal laminates: part 2: the forming properties*. 1994, Delft University of Technology

32. Beumler T (2004) *Flying GLARE: a contribution to aircraft certification issues in strength properties in non-damaged and fatigue damaged GLARE structures*. Delft University Press
33. Kim D, Ramulu M, Pedersen W (2005) Machinability of titanium/graphite hybrid composites in drilling. Trans NAMRI/SME 33: 445–452
34. Kim D, Ramulu M (2007) Study on the drilling of titanium/graphite hybrid composites. J Eng Mater Technol 129(3):390–396
35. Kim GW, Lee KY (2005) Critical thrust force at propagation of delamination zone due to drilling of FRP/metallic strips. Compos Struct 69(2):137–141
36. Sánchez Carrilero M, Álvarez M, Ares E, Astorga J, Cano M, Marcos M (2006) *Dry drilling of fiber metal laminates CF/AA2024. A preliminary study*. in *Materials science forum*. Trans Tech Publ
37. Pawar OA, Gaikhe YS, Tewari A, Sundaram R, Joshi SS (2015) Analysis of hole quality in drilling GLARE fiber metal laminates. Compos Struct
38. Senthilkumar, B.M.A., *Mechanical and machinability characteristics of fiber metal laminates*. 2016: LAP Lambert Academic Publishing 60
39. Rezende BA, Silveira ML, Vieira LM, Abrão AM, Faria PEd, Rubio JCC (2016) Investigation on the effect of drill geometry and pilot holes on thrust force and burr height when drilling an aluminium/PE sandwich material. Materials 9(9):774
40. Devi GR and Palanikumar K (2018) Analysis on drilling of woven glass fibre reinforced aluminium sandwich laminates. J Mater Res Tech
41. Coesel JFW (1994) *Drilling of fibre-metal laminates*, in *Faculty of aerospace engineering*. Delft University of Technology p 63
42. Park SY, Choi WJ, Choi CH, Choi HS (2017) Effect of drilling parameters on hole quality and delamination of hybrid GLARE laminate. Compos Struct
43. Sureshkumar M, Lakshmanan D, and Murugarajan A (2014) Experimental investigation and mathematical modelling of drilling on GFRP composites. Mater Res Innov 18(S1): S1-94-S1-97
44. Vankanti VK, Ganta V (2014) Optimization of process parameters in drilling of GFRP composite using Taguchi method. J Mater Res Tech 3(1):35–41
45. Krishnaraj V, Prabukarthi A, Ramanathan A, Elanghovan N, Senthil Kumar M, Zitoune R, Davim JP (2012) Optimization of machining parameters at high speed drilling of carbon fiber reinforced plastic (CFRP) laminates. Compos Part B 43(4):1791–1799
46. Ameur M, Habak M, Kenane M, Aouici H, Cheikh M (2017) Machinability analysis of dry drilling of carbon/epoxy composites: cases of exit delamination and cylindricity error. Int J Adv Manuf Technol 88(9–12):2557–2571
47. Zitoune R, Krishnaraj V, Collombet F (2010) Study of drilling of composite material and aluminium stack. Compos Struct 92(5): 1246–1255
48. Sreenivasulu R (2015) Optimization of burr size, surface roughness and circularity deviation during drilling of Al 6061 using Taguchi design method and artificial neural network. Independent Journal of Management & Production 6(1):093–108
49. Giasin K, Gorey G, Byrne C, Sinke J, Brousseau E (2019) Effect of machining parameters and cutting tool coating on hole quality in dry drilling of fibre metal laminates. Compos Struct
50. Giasin K, Ayvar-Soberanis S (2017) Microstructural investigation of drilling induced damage in fibre metal laminates constituents. Compos A: Appl Sci Manuf 97:166–178
51. Phadnis VA, Makhdum F, Roy A, Silberschmidt VV (2013) Drilling in carbon/epoxy composites: experimental investigations and finite element implementation. Compos A: Appl Sci Manuf 47: 41–51
52. Dumkum C, Jaritngam P, Tangwarodomnukun V (2019) Surface characteristics and machining performance of TiAlN-, TiN-and AlCrN-coated tungsten carbide drills. Proc Inst Mech Eng B J Eng Manuf 233(4):1075–1086
53. Abdelhafeez AM, Soo SL, Aspinwall DK, Dowson A, Arnold D (2015) Burr formation and hole quality when drilling titanium and aluminium alloys. Procedia CIRP 37:230–235
54. Davim JP (2013) *Machining composites materials*. John Wiley & Sons
55. Sultan A, Sharif S, Kurniawan D (2015) Effect of machining parameters on tool wear and hole quality of AISI 316L stainless steel in conventional drilling. Procedia Manufacturing 2:202–207
56. Stephenson DA and Agapiou JS (2005) *Metal cutting theory and practice*. Vol. 68. CRC press
57. Gardiner G. (2014) *Hole quality defined*. compositesworld
58. SANDVIK, Improved hand-held hole making in composites. 2011: http://www.sandvik.coromant.com
59. AlSi I (2017) Effect of cutting parameters on the drilling of AlSi7 metallic foams. Materiali in tehnologije 51(1):19–24
60. Hayajneh MT (2001) Hole quality in deep hole drilling. Mater Manuf Process 16(2):147–164
61. Islam MN and Boswell B (2016) *Effect of cooling methods on hole quality in drilling of aluminium 6061-6T*. in *IOP Conference Series: Materials Science and Engineering*. IOP Publishing
62. Sheikh-Ahmad, J.Y., *Machining of polymer composites*. 2009: Springer
63. Tsao C, Hocheng H (2005) Effects of exit back-up on delamination in drilling composite materials using a saw drill and a core drill. Int J Mach Tools Manuf 45(11):1261–1270

Publisher's note Springer Nature remains neutral with regard to jurisdictional claims in published maps and institutional affiliations.